

Superconductivity around nematic quantum critical point in two-dimensional metals

Guo-Zhu Liu^{1,*} and Jing-Rong Wang²

¹*Department of Modern Physics, University of Science and Technology of China, Hefei, Anhui 230026, P. R. China*

²*Anhui Province Key Laboratory of Condensed Matter Physics at Extreme Conditions, High Magnetic Field Laboratory of the Chinese Academy of Science, Hefei, Anhui 230031, P. R. China*

We study the properties of s -wave superconductivity induced around a nematic quantum critical point in two-dimensional metals. The strong Landau damping and the Cooper pairing between incoherent fermions have dramatic mutual influence on each other, and hence should be treated on an equal footing. This problem is addressed by analyzing the self-consistent Dyson-Schwinger equations for the superconducting gap and Landau damping rate. We solve the equations at zero temperature without making any linearization, and show that the superconducting gap is maximized at the quantum critical point and decreases rapidly as the system departs from this point. The interplay between nematic fluctuation and an additional pairing interaction, caused by phonon or other boson mode, is also investigated. The total superconducting gap generated by such interplay can be several times larger than the direct sum of the gaps separately induced by these two pairing interactions. This provides a promising way to achieve remarkable enhancement of superconductivity.

PACS numbers: 71.10.Hf, 74.20.Mn, 74.25.Dw, 74.40.Kb

I. INTRODUCTION

Conventional superconductors are well described by the Bardeen-Cooper-Schrieffer (BCS) theory [1], which gives a microscopic mechanism for the superconducting (SC) transition and a reliable quantitative estimate for the SC gap Δ and critical temperature T_c when the electron-phonon coupling is not strong. BCS theory and its later extension by Eliashberg [2] are firmly based on the validity of Fermi liquid (FL) theory [3] that is known to be perfectly applicable to normal metals. When a net attraction is achieved, Cooper pairing is realized, driving the SC phase transition.

The discovery of superconductivity in heavy fermion materials [4], cuprates [5–7], and iron pnictides [8–12] has stimulated intensive research activities in the past four decades. Many of these superconductors exhibit two salient universal features: the existence of a SC dome with a maximal T_c ; the emergence of non-FL behavior in the non-SC phase. A great challenge of condensed matter physics is to develop a unified framework to account for these two features [4–11]. Based on existing experiments, it is broadly expected that the observed NFL behavior and dome-shaped SC boundary might be caused by certain quantum critical point (QCP). However, although this scenario seems very promising, it proves very difficult to determine the intrinsic correlation among the quantum criticality, NFL behavior, and SC dome. Another unusual, but less universal, feature is that, T_c can be much higher in some cuprates and iron-based superconductors than ordinary phonon-mediated superconductors. While in principle Cooper pairing could be induced by several possible bosonic modes, such as phonon, magnetic fluctuation, and nematic fluctuation, none of them is able to

account for all the basic features observed in experiments.

In this paper, we study the fate of superconductivity formed in a two-dimensional (2D) metal that is tuned close to a nematic quantum phase transition [13–29]. Such model system has wide applications since electronic nematicity has already been observed in some cuprates [6, 7] and almost all iron-based superconductors [8–12]. A special material is FeSe [12, 30–32]: it exhibits a clear nematic order; no magnetic order is observed; the non-SC state is a NFL; T_c is below 9K but significantly enhanced via K intercalation to reach 40-60K; there is a SC dome with T_c being maximal near nematic QCP. It is natural to expect that nematic order plays an essential role in the formation of superconductivity in this material.

For a 2D metal, the quantum nematic fluctuation can lead to both strong NFL behavior and Cooper pairing. There is a complicated mutual influence between NFL behavior and Cooper pairing: strong Landau damping shortens the fermion lifetime and accordingly may affect the possibility of Cooper pairing; nonzero SC gap reduces the space of final states into which fermions are scattered and hence weakens the NFL behavior. It is hard to judge whether NFL behavior favors superconductivity without doing concrete calculations. Since the BCS-Eliashberg method become invalid in the NFL regime, it is necessary to employ a generalized framework so that NFL behavior and Cooper pairing can be treated on an equal footing.

We will address the above issue by using the Dyson-Schwinger (DS) integral equation approach, which is more general than BCS-Eliashberg method. We first construct a set of self-consistently coupled DS equations for the wave renormalization function and the SC gap, and then solve them in an unbiased way. We are especially interested in the magnitude of the SC gap, which could be measured by experiments, including angle-resolved photoemission spectroscopy and scanning tunneling microscope. For this purpose, we do not make the linearizing approximation, which is valid only when $T \approx T_c$, but

*Corresponding author: gzliu@ustc.edu.cn

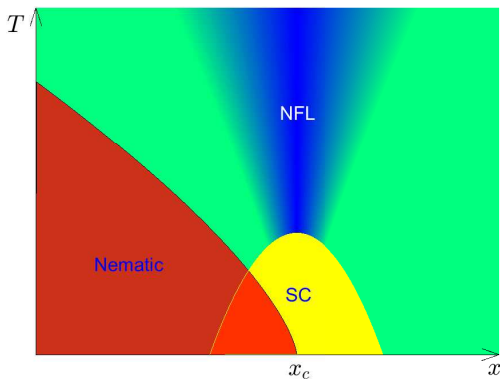


FIG. 1: Schematic phase diagram on the x - T plane. We use $r = x - x_c$ to denote the tuning parameter. The non-SC ground state is a normal FL at large r , and a NFL at small r . SC gap is strongly peaked at QCP.

directly solve the nonlinear DS equations. Based on the solutions, the damping rate, SC gap, and their mutual influence can be simultaneously determined. The vertex correction is simply neglected in BCS-Eliashberg treatment. In our DS equation calculation, we introduce a suitable *ansatz* of the vertex correction, and demonstrate that it can lead to substantial influence on the gap size. Moreover, we also incorporate the feedback of SC gap on the effective nematic propagator. The gap strongly suppresses the low-energy DOS and strengthens the nematic fluctuation, which enhances superconductivity.

After performing extensive calculations, we find that, the SC gap is strongly peaked at the nematic QCP and rapidly suppressed as the system moves away from the QCP into the disordered phase. There is a clear dome-shaped curve of the SC gap, which is schematically shown in Fig. 1. Near the QCP, the NFL behavior is hidden at energy scales below the SC gap, but may show its existence at intermediate energy scales. We thus obtain a quantitative description of the complicated correlation among nematic QCP, NFL behavior, SC dome, and high T_c , which might be applicable to doped FeSe and some cuprates.

Another crucial issue is to obtain a high, substantially enhanced T_c . This can be naturally realized if we could find an efficient way to promote the SC gap Δ . We will study the interplay between the nematic fluctuation and an additional pairing interaction, which might arise from phonon or other type of bosonic mode. A remarkable result is that the total gap generated by this interplay is several times larger than the direct sum of the gaps induced by two pairing mechanisms separately. Consequently, the corresponding T_c would be much larger than that produced by one single pairing mechanism.

The rest of the paper is structures as follows. The model is given in Sec. II, and the self-consistent DS equations are derived in Sec. III. The solutions of DS equations are presented and systematically analyzed in Sec. IV. The main results are summarized in Sec. V.

II. MODEL HAMILTONIAN

We consider a 2D metal at the border of nematic transition. The low-energy effective model for a 2D metal close to a nematic QCP is given by [16, 19, 20, 33–38]

$$L_\psi = \psi_{+\alpha}^\dagger \left(\partial_\tau - iv\partial_x - \frac{1}{2m}\partial_y^2 \right) \psi_{+\alpha} + \psi_{-\alpha}^\dagger \left(\partial_\tau + iv\partial_x - \frac{1}{2m}\partial_y^2 \right) \psi_{-\alpha}, \quad (1)$$

$$L_\phi = \frac{N}{2e^2} (\partial_y \phi)^2 + \frac{N_f r}{2} \phi^2, \quad (2)$$

$$L_{\psi\phi} = \phi \left(\psi_{+\alpha}^\dagger \psi_{+\alpha} + \psi_{-\alpha}^\dagger \psi_{-\alpha} \right), \quad (3)$$

$$L_{4f} = -\lambda \psi^\dagger \psi^\dagger \psi \psi. \quad (4)$$

Here, L_ψ and L_ϕ are the Lagrangian densities for the fermion field ψ and the Ising-type nematic order parameter ϕ , respectively. The Yukawa coupling between ψ and ϕ is described by $L_{\psi\phi}$. There is an additional short-ranged BCS coupling term, given by L_{4f} , which might be induced by exchanging phonons. We use v to denote the Fermi velocity and m the fermion mass. The $+$ and $-$ signs appearing in the fermion field $\psi_{+,-}$ stand for the fermion excitations around two patches near $\pm \mathbf{k}_F$ [16, 19, 20, 33–38]. Moreover, $\alpha = 1, 2, \dots, N$ represents the fermion flavor. The physical fermion flavor is $N = 2$, corresponding to the two spin components.

To make this paper self-contained, we first sketch the computation of the polarization function. The free fermion propagator is given by

$$G_s(\omega, \mathbf{k}) = \frac{1}{-i\omega + \xi_{\mathbf{k}}^s}, \quad (5)$$

where $\xi_{\mathbf{k}}^s = \frac{k^2}{2m}$ with m being the fermion mass. At the Fermi surface, $\xi_{\mathbf{k}}^s$ can be simplified to

$$\xi_{\mathbf{k}}^s = svk_x + \frac{k_y^2}{2m}, \quad (6)$$

where k_x is the tangential component of momentum and k_y the perpendicular component. To the leading order of perturbative expansion, the polarization is defined as

$$\Pi(\Omega, \mathbf{q}) = N \sum_{s=\pm 1} \int \frac{d\omega}{2\pi} \frac{d^2 \mathbf{k}}{(2\pi)^2} G_s(\omega, \mathbf{k}) \times G_s(\omega + \Omega, \mathbf{k} + \mathbf{q}). \quad (7)$$

This integral has already been computed in previous works, and it is well-known that [16, 19, 20, 33–38]

$$\Pi(\Omega, \mathbf{q}) = -\frac{N}{2\pi^2} \frac{m}{v|q_y|} 2\pi i \text{sgn}(\Omega) i\Omega = N\gamma \frac{|\Omega|}{|q_y|}, \quad (8)$$

where $\gamma = \frac{m}{\pi v}$. The dressed propagator of nematic field ϕ has the form

$$D(\omega, \mathbf{q}) = \frac{1}{N \left(\frac{q_y^2}{e^2} + \gamma \frac{|\Omega|}{|q_y|} + r \right)}, \quad (9)$$

which is independent of q_x . We have introduced a tuning parameter r to measure the distance of the system from the nematic QCP. Depending on the material, r could be doping concentration, pressure, or external field. The nematic QCP is defined as $r = 0$. Here, we approach to the QCP from the disordered phase, with r decreasing from certain finite value down to zero continuously. The ordered phase of nematic transition is more complicated, and thus we leave for future work.

III. SELF-CONSISTENT DYSON-SCHWINGER EQUATIONS

The Yukawa interaction between gapless fermions and nematic fluctuation can give rise to both strong Landau damping and Cooper pairing. To study this problem, it is most convenient to define a standard Nambu spinor:

$$\Psi(\omega, \mathbf{k}) = \begin{pmatrix} \psi_\uparrow(\omega, \mathbf{k}) \\ \psi_\downarrow^\dagger(-\omega, -\mathbf{k}) \end{pmatrix}. \quad (10)$$

Its conjugate is

$$\Psi^\dagger(\omega, \mathbf{k}) = \left(\psi_\uparrow^\dagger(\omega, \mathbf{k}) \quad \psi_\downarrow(-\omega, -\mathbf{k}) \right). \quad (11)$$

For an ordinary FL (good) metal, one can write down the following mean-field Lagrangian

$$\mathcal{L} = \Psi^\dagger \begin{pmatrix} i\omega_n - \xi_{\mathbf{k}} & \Delta \\ \Delta^* & i\omega_n + \xi_{\mathbf{k}} \end{pmatrix} \Psi, \quad (12)$$

where $\Delta \propto \langle \psi_\uparrow \psi_\downarrow \rangle$ is an s -wave SC gap. It is then easy to have a normal and an anomalous Green's function:

$$\mathcal{G}(\omega_n, \mathbf{k}) = \frac{i\omega_n + \xi_{\mathbf{k}}}{\omega_n^2 + \xi_{\mathbf{k}}^2 + \Delta^2}, \quad (13)$$

$$\mathcal{F}(\omega_n, \mathbf{k}) = \frac{\Delta}{\omega_n^2 + \xi_{\mathbf{k}}^2 + \Delta^2}. \quad (14)$$

The corresponding SC gap equation has the form

$$\Delta = \lambda T \sum_{\omega_n} \int \frac{d^d \mathbf{k}}{(2\pi)^d} \mathcal{F}(\omega_n, \mathbf{k}). \quad (15)$$

$$= \lambda T \sum_{\omega_n} \int \frac{d^d \mathbf{k}}{(2\pi)^d} \frac{\Delta}{\omega_n^2 + \xi_{\mathbf{k}}^2 + \Delta^2}, \quad (16)$$

with λ being the strength parameter for the attractive force. We here focus on the case of $d = 2$ spatial dimension, but the extension to $d = 3$ is straightforward. The SC gap can be easily obtained by solving this equation.

When a 2D metal is tuned on the border of long-range nematic order, it becomes a bad metal due to the coupling of gapless fermions with quantum critical nematic fluctuation. As the tuning parameter r grows, driving the system to depart from nematic QCP, the NFL behavior is gradually weakened. At finite r , the system exhibits

normal FL behavior at energy scales well below r and unusual NFL behavior at energy scale well above r . When the energy scale becomes sufficiently large, the quantum nematic fluctuation disappears. Thus, for finite r , NFL behavior actually emerges within an intermediate range of energy scale. For very large r , the range for NFL behavior to show up becomes extremely narrow, and thus can be neglected. In this case, the mean-field Hamiltonian (12) is definitely no longer sufficient to capture the complicated mutual influence between FL behavior, NFL behavior, and Cooper pairing. However, it is possible to properly generalize (12) so as to describe the SC pairing in both the FL and NFL regimes. For this purpose, we write the normal and anomalous Green's functions in the following generic forms:

$$\mathcal{G}'(\omega_n, \mathbf{k}) = \frac{A_1(\omega_n, \mathbf{k})\omega_n + A_2(\omega_n, \mathbf{k})\xi_{\mathbf{k}}}{\Xi(\omega_n, \mathbf{k})}, \quad (17)$$

$$\mathcal{F}'(\omega_n, \mathbf{k}) = \frac{\Delta(\omega_n, \mathbf{k})}{\Xi(\omega_n, \mathbf{k})}. \quad (18)$$

where

$$\Xi(\omega_n, \mathbf{k}) = A_1^2(\omega_n, \mathbf{k})\omega_n^2 + A_2^2(\omega_n, \mathbf{k})\xi_{\mathbf{k}}^2 + \Delta^2(\omega_n, \mathbf{k}).$$

Here, $A_{1,2}(\omega_n, \mathbf{k})$ are two renormalization functions. The interaction-induced Landau damping is encoded in the wave renormalization function $A_1(\omega_n, \mathbf{k})$. It is interesting that $A_1(\omega_n, \mathbf{k})$ exhibits distinct behaviors in NFL, FL, and fully gapped SC phases. For a NFL, $A_1(\omega_n, \mathbf{k})$ increases rapidly as the energy is lowered, and eventually diverges in the zero-energy limit. For a FL, $A_1(\omega_n, \mathbf{k})$ is convergent at low energies. When superconductivity is induced in a NFL metal, $A_1(\omega_n, \mathbf{k})$ approaches a finite value at energies below the SC gap, but can still display NFL-like behaviors in an intermediate range of energies. The fermion mass renormalization can be obtained from $A_1(\omega_n, \mathbf{k})$ and $A_2(\omega_n, \mathbf{k})$. Apparently, now $\mathcal{G}'(\omega_n, \mathbf{k})$ and $\mathcal{F}'(\omega_n, \mathbf{k})$ contain three important interaction-induced effects: strong Landau damping, mass renormalization, and SC gap generation. The functions $A_{1,2}(\omega_n, \mathbf{k})$ and $\Delta(\omega_n, \mathbf{k})$ satisfy the following self-consistent DS integral equations:

$$\begin{aligned} A_1(\varepsilon_n, \mathbf{p})\varepsilon_n &= \varepsilon_n + \int_{\omega_n, \mathbf{k}} A_1(\omega_n, \mathbf{k})\omega_n F(\varepsilon_n, \mathbf{p}, \omega_n, \mathbf{k}), \\ A_2(\varepsilon_n, \mathbf{p})\xi_{\mathbf{p}} &= \xi_{\mathbf{p}} + \int_{\omega_n, \mathbf{k}} A_2(\omega_n, \mathbf{k})\xi_{\mathbf{k}} F(\varepsilon_n, \mathbf{p}, \omega_n, \mathbf{k}), \\ \Delta(\varepsilon_n, \mathbf{p}) &= \int_{\omega_n, \mathbf{k}} \Delta(\omega_n, \mathbf{k}) F(\varepsilon_n, \mathbf{p}, \omega_n, \mathbf{k}) \\ &\quad + \lambda \int_{\omega_n, \mathbf{k}} \frac{\Delta(\omega_n, \mathbf{k})}{\Xi(\omega_n, \mathbf{k})}, \end{aligned} \quad (19)$$

where $\int_{\omega_n, \mathbf{k}} \equiv T \sum_{\omega_n} \int \frac{d^2 \mathbf{k}}{(2\pi)^2}$ and

$$F(\varepsilon_n, \mathbf{p}, \omega_n, \mathbf{k}) = \frac{\Gamma(\varepsilon_n, \mathbf{p}; \omega_n, \mathbf{k})}{\Xi(\omega_n, \mathbf{k})} D(\varepsilon_n - \omega_n, \mathbf{p} - \mathbf{k}). \quad (20)$$

From these equations, we can see that the nematic fluctuation contributes to both $A_{1,2}(\omega_n, \mathbf{k})$ and $\Delta(\omega_n, \mathbf{k})$, whereas the BCS attraction makes no contribution to $A_{1,2}(\omega_n, \mathbf{k})$. In traditional BCS-Eliashberg scheme for strongly coupled superconductors, the vertex corrections are unimportant due to Migdal theorem. The validity of this theorem relies on the fact that the fermion mass is much smaller than the lattice mass. In the present case, there is no guarantee that the vertex correction to the Yukawa coupling is unimportant. In order not to underestimate the importance of vertex correction, we have introduced a vertex function $\Gamma(\varepsilon_n, \mathbf{p}; \omega_n, \mathbf{k})$. In the most generic case, the vertex $\Gamma(\varepsilon, \mathbf{p}; \omega, \mathbf{k})$ also satisfies an integral equation that couples consistently to those of $A_{1,2}(\varepsilon, \mathbf{p})$ and $\Delta(\varepsilon, \mathbf{p})$. This would make the analysis practically impossible. We will alternatively introduce some suitable *Ansatz* for the vertex function.

The three DS equations are intimately coupled to each other, reflecting the fact that Landau damping effect, fermion mass renormalization, and Cooper pairing have significant mutual influence. It is thus difficult to perform numerical evaluations. In the following, we will employ several further approximations. The first approximation is to take the zero temperature limit by employing the replacement $T \sum_{\omega_n} \rightarrow \int_{-\infty}^{+\infty} \frac{d\omega}{2\pi}$. Since the dressed nematic propagator $D(\varepsilon, \mathbf{p})$ does not depend on q_x , the functions $A_{1,2}(\omega, \mathbf{k})$ are independent of k_x and thus can be written as $A_{1,2}(\omega, k_y)$. Accordingly, the vertex function is expressed in the form $\Gamma(\varepsilon_n, p_y; \omega_n, k_y)$. Now the above self-consistent equations can be simplified to

$$\begin{aligned} A_1(\varepsilon, p_y)\varepsilon &= \varepsilon + \int_{\omega, k_x, k_y} A_1(\omega, k_y)\omega F(\varepsilon, p_y, \omega, k_y), \\ A_2(\varepsilon, p_y)\xi_{\mathbf{p}} &= \xi_{\mathbf{p}} + \int_{\omega, k_x, k_y} A_2(\omega, k_y)v k_x F(\varepsilon, p_y, \omega, k_y), \\ A_3(\varepsilon, p_y)\Delta &= \int_{\omega, k_x, k_y} \Delta(\omega, k_y)F(\varepsilon, p_y, \omega, k_y) \\ &\quad + \lambda \int_{\omega, k_x, k_y} \frac{\Delta(\omega, k_y)}{\Xi(\omega, k_y)}, \end{aligned} \quad (21)$$

where

$$F(\varepsilon, p_y, \omega, k_y) = \frac{\Gamma(\varepsilon, p_y; \omega, k_y)}{\Xi(\omega, k_y)} D(\varepsilon - \omega, p_y - k_y),$$

and

$$\Xi(\omega, k_y) = A_1^2(\omega, k_y)\omega^2 + A_2^2(\omega, k_y)v^2 k_x^2 + \Delta^2(\omega, k_y).$$

Here, we use the notation $\int_{\omega, k_x, k_y} \equiv \int \frac{d\omega}{2\pi} \frac{dk_x}{2\pi} \frac{dk_y}{2\pi}$. A transformation $vk_x + \frac{1}{2m}k_y^2 \rightarrow vk_x$ has been utilized. It is now easy to verify that

$$A_2(\varepsilon, p_y) = 1. \quad (22)$$

After performing the integration of k_x , we obtain

$$\begin{aligned} A_1(\varepsilon, p_y)\varepsilon &= \varepsilon + \frac{1}{2v} \int \frac{d\omega}{2\pi} \frac{dk_y}{2\pi} A_1(\omega, k_y)\omega F_1(\varepsilon, p_y, \omega, k_y), \\ \Delta(\varepsilon, p_y) &= \frac{1}{2v} \int \frac{d\omega}{2\pi} \frac{dk_y}{2\pi} \Delta(\omega, k_y)F_1(\varepsilon, p_y, \omega, k_y) \\ &\quad + \frac{\lambda}{2v} \int \frac{d\omega}{2\pi} \frac{dk_y}{2\pi} \frac{\Delta(\omega, k_y)}{J_1(\omega, k_y)}, \end{aligned} \quad (23)$$

where

$$\begin{aligned} F_1(\varepsilon, p_y, \omega, k_y) &= \frac{\Gamma(\varepsilon, p_y; \omega, k_y)}{J_1(\omega, k_y)} D(\varepsilon - \omega, p_y - k_y), \\ J_1(\omega, k_y) &= \sqrt{A_1^2(\omega, k_y)\omega^2 + \Delta^2(\omega, k_y)}. \end{aligned}$$

The vertex function needs to be specified at this stage. The simplest choice is to adopt the bare vertex, i.e.,

$$\Gamma(\varepsilon, p_y; \omega, k_y) = 1. \quad (24)$$

This approximation is widely used in the BCS-Eliashberg treatment of superconducting pairing [13, 20], but is apparently oversimplified. Here, we choose to consider the following *Ansatz*:

$$\Gamma(\varepsilon, p_y; \omega, k_y) = \frac{1}{2} [A_1(\varepsilon, p_y) + A_1(\omega, k_y)], \quad (25)$$

which is symmetric under the exchange of energy-momentum variables.

We further suppose that the dependence of A_1 and Δ on component p_y is weak, namely

$$A_1(\varepsilon, p_y) \rightarrow A_1(\varepsilon), \quad \Delta(\varepsilon, p_y) \rightarrow \Delta(\varepsilon). \quad (26)$$

Here, we use the Fermi momentum k_F to serve as the cutoff for k_y . Now, the integration over k_y appearing in the first term of the gap equation in Eq. (23) is convergent and can be carried out directly. For the rest terms of Eq. (23), we define $|k_y| = (e^2\gamma|\varepsilon - \omega|)^{1/3}x$ and then find that

$$\begin{aligned} A_1(\varepsilon)\varepsilon &= \varepsilon + \frac{g\omega_c^{1/3}}{N} \int_0^{\omega_c} d\omega A_1(\omega)\omega \\ &\quad \times [F_3(\varepsilon - \omega) - F_3(\varepsilon + \omega)], \end{aligned} \quad (27)$$

$$\begin{aligned} \Delta(\varepsilon) &= \frac{g\omega_c^{1/3}}{N} \int_0^{\omega_c} d\omega \Delta(\omega) [F_3(\varepsilon - \omega) + F_3(\varepsilon + \omega)] \\ &\quad + \lambda' \int_0^{\omega_c} d\omega \frac{\Delta(\omega)}{J_2(\omega)}, \end{aligned} \quad (28)$$

where

$$\begin{aligned} F_3(\varepsilon \pm \omega) &= \frac{\Gamma(\varepsilon; \omega)}{J_2(\omega)} \frac{1}{|\varepsilon \pm \omega|^{1/3}} \frac{3\sqrt{3}}{2\pi} \\ &\quad \times \int_0^{+\infty} dx \frac{x}{x^3 + 1 + \left(\frac{e}{\gamma|\varepsilon \pm \omega|}\right)^{2/3} r x} \end{aligned} \quad (29)$$

with $J_2(\omega) = \sqrt{A_1^2(\omega)\omega^2 + \Delta^2(\omega)}$. We have used the relations $A_1(\omega) = A_1(-\omega)$ and $\Delta(\omega) = \Delta(-\omega)$, and defined new parameters

$$\lambda' = \frac{\lambda k_F}{2\pi^2 v}, \quad g = \frac{e^{4/3}}{6\sqrt{3}\pi v \gamma^{1/3} \omega_c^{1/3}}. \quad (30)$$

The upper limit of x is taken to be infinity, which is justified because the integration over x is free of divergence. From Eqs. (27) and (28), we can see that $1/N$ can serve as an effective expanding parameter for the fermion-nematic interaction.

The equations (27) and (28) are applicable to both the FL regime and NFL regime, and also can capture the FL-to-NFL crossover tuned by changing the energy scale, which allows us to examine the mutual influence between Landau damping and Cooper pairing as the system is approaching the nematic QCP. At exactly the nematic QCP, $r = 0$ and we have

$$\begin{aligned} A_1(\varepsilon)\varepsilon &= \varepsilon + \frac{g\omega_c^{1/3}}{N} \int_0^{\omega_c} d\omega A_1(\omega)\omega K_-(\varepsilon, \omega), \quad (31) \\ \Delta(\varepsilon) &= \frac{g\omega_c^{1/3}}{N} \int_0^{\omega_c} d\omega \Delta(\omega)K_+(\varepsilon, \omega) \\ &\quad + \lambda' \int_0^{\omega_c} d\omega \frac{\Delta(\omega)}{J_2(\omega)}, \quad (32) \end{aligned}$$

where

$$K_{\pm}(\varepsilon, \omega) = \frac{\Gamma(\varepsilon; \omega)}{J_2(\omega)} \left(\frac{1}{|\varepsilon - \omega|^{1/3}} - \frac{1}{|\varepsilon + \omega|^{1/3}} \right). \quad (33)$$

By solving the two equations self-consistently, we can get the Landau damping rate, from $A_1(\varepsilon)$, and SC gap.

Our DS equations are quite general, and contain all the essential information for Landau damping and Cooper pairing. They should recover the results obtained previously in limiting cases. If the nematic QCP is removed, $A_1 \equiv 1$, the DS equations are simply reduced to the well-known BCS gap equation. An opposite limit is reached by taking $\Delta = 0$, corresponding to the non-SC ground state. In this case, the quantum nematic fluctuation leads to strong fermion damping effect. After neglecting the vertex correction, we obtain

$$A_1(\varepsilon)\varepsilon \approx \varepsilon + \frac{6g\omega_c^{1/3}}{N}\varepsilon^{2/3} \quad (34)$$

in the low-energy region $\varepsilon \ll \omega_c$. This is a typical NFL behavior, and well consistent with the results reported previously [33–38].

IV. SOLUTIONS OF COUPLED EQUATIONS

In the limiting case with $\Delta = 0$, the system exhibits well-known NFL behavior $(A_1 - 1)\varepsilon \propto \varepsilon^{2/3}$ at $r = 0$. At nonzero r , there is a crossover from NFL regime to normal

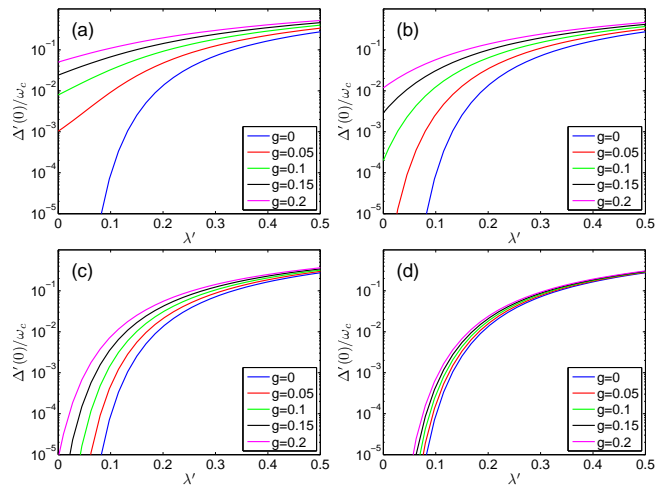


FIG. 2: Dependence of zero-energy SC gap on tuning parameter r' . The energy scale is given by $\omega_c = \mu_F$. (a) $r' = 0$; (b) $r' = 1$; (c) $r' = 10$; (d) $r' = 100$. The re-scaled parameter $r' = e^{2/3}r/(\gamma\omega_c)^{2/3}$ represents an effective mass of nematic order parameter. The QCP is located at $r' = 0$.

FL regime as r or the energy scale is varied. Cooper pairing is formed on the basis of the NFL metal near nematic QCP.

To obtain a quantitatively precise relation between the Landau damping rate and SC gap at $T = 0$, the coupled DS equations in (21) cannot be linearized. The linearization approximation is valid only in the close vicinity of T_c . Moreover, it is not appropriate to first perturbatively compute $A_1(\varepsilon, p)$ and then to use the perturbative result to solve the gap equation, because this would miss the important suppressing effect of SC gap on the Landau damping. In this work, we have solved the equations in (21) in a self-consistent and entirely unbiased way, and determine $A_1(\varepsilon, p)$ and $\Delta(\varepsilon, p)$ simultaneously. To make numerical calculation simpler, we temporarily ignore the dependence of these function on momenta, and compute $A_1(\varepsilon)$ and $\Delta(\varepsilon)$. The influence of momentum-dependence will be examined below.

Currently, we concentrate on the nematic QCP and the disordered phase, corresponding to the parameter range $r \geq 0$. In the region with $r < 0$, the SC and nematic orders are expected to coexist. These two orders might compete, which makes theoretical treatment more involved than the case of $r \geq 0$. This problem will be considered in future work.

A. Superconducting dome

In Fig. 2, we present the zero-energy SC gap obtained at various values of g , λ' , and r' . At $r' = 0$, the SC gap $\Delta(0)$ obtained at $\lambda' = 0.1$ and $g = 0.2$ is roughly one hundred times larger than that obtained at $\lambda' = 0.1$ and $g = 0$. As g grows, the gap $\Delta(0)$ further increases. At $r' = 1$, the enhancement is still dramatic. As r' contin-

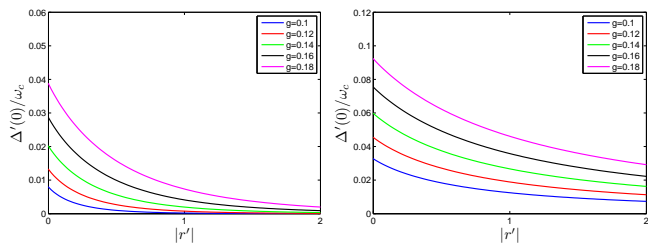


FIG. 3: Scaled zero-energy SC gap $\Delta'(\omega) = \Delta(\omega)/A_1(\omega)$ is maximized at $r = 0$ and is strongly suppressed by growing r . We take $\lambda = 0$ in (a) and $\lambda = 0.1$ in (b). The presence of a small λ greatly amplifies the gap size.

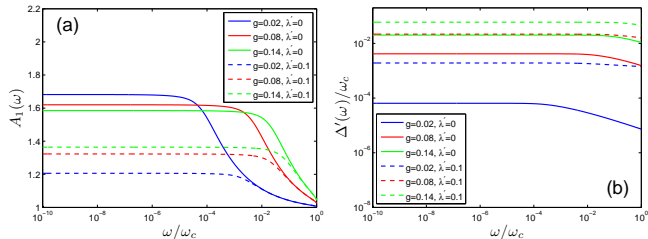


FIG. 4: Dependence of $A_1(\omega)$ and $\Delta(\omega)$ on ω are shown in (a) and (b), respectively.

ues growing, the enhancement is rapidly weakened, and finally nearly disappears when r' is large enough. It is therefore clear that the nematic-induced enhancement of SC gap is most significant at the QCP.

The quantum nematic fluctuation itself can trigger Cooper pairing even though there is no net attraction induced by other scenarios, consistent with previous works [13, 16]. As can be seen from Fig. 2, a finite SC gap is opened at $\lambda' = 0$, and $\Delta(0)$ is an increasing function of g , the Yukawa coupling. This gap is strongly peaked at the QCP with $r' = 0$, and decreases rapidly as r' grows. In case a net attraction with strength λ' already develops, presumably due to commonly existing phonons, the SC gap is significantly enhanced. Normally, λ' only has weak dependence on r' , thus the gap is still peaked at the QCP. All these results are summarized in Fig. 3. An apparent conclusion is that there emerges a dome-shaped boundary of the SC phase with the maximal gap appearing at nematic QCP.

The energy dependence of $A_1(\omega)$ and $\Delta(\omega)$ is shown in Fig. 4. In the low-energy region, corresponding to small values of ω , $A_1(\omega)$ is nearly a constant. The reason for this feature is that the SC gap substantially reduces the space of final states into which the fermions are scattered by the nematic fluctuation. The SC gap can be

considered as an infrared cutoff, and the original singular increasing of A_1 is prevented in the energy scale lower than the SC gap. It is easy to observe from Fig. 4 that $A_1(\omega)$ is dramatically suppressed when ω/ω_c exceeds certain threshold, implying the emergence of strong Landau damping effect and, accordingly, unusual NFL behavior. Above T_c , the gap is closed due to thermal fluctuations, and the system enters from SC phase into a finite- T NFL phase. If r' takes an intermediate value, the system is in a mixed FL/NFL regime: the NL and NFL behaviors show up at different energy scales. All these complicated properties can be quantitatively reproduced from the self-consistent solutions of DS equations.

B. Importance of vertex correction

We now consider the impact of the vertex correction to Yukawa coupling between fermion and nematic order. The DS equations are solved with and without vertex correction respectively, with the results being given in Fig. 5. Comparing Fig. 5 to Fig. 2, we find that including the vertex correction does not change the qualitative results obtained by adopting the bare vertex. However, the vertex correction leads to considerable enhancement of superconductivity. If the vertex correction is ignored, the magnitude of SC gap would be underestimated. Our results indicate that the vertex correction is important only at small values of r' , namely in the close vicinity of nematic QCP where the Yukawa coupling is singular. If the system is far from the nematic QCP, it is valid to ignore the vertex correction, and the SC transition could be described by the BCS-Eliashberg method.

C. Including gap in the polarization

The SC gap size replies sensitively on the effective strength of Yukawa coupling. The free propagator of nematic fluctuation is $\propto q^{-2}$ at QCP. Such interaction is effectively long-ranged. The collective particle-hole excitations weakens such singular interaction, which is reflected by the polarization $\Pi(\Omega, \mathbf{q})$. In the above calculations, we have used the expression of $D(\Omega, \mathbf{q})$ given by Eq. (9). The feedback effect of SC gap on $D(\Omega, \mathbf{q})$ needs to be carefully examined. Intuitively, the SC gap suppresses the low-energy DOS of fermions, which is expected to weaken the screening effect and increase the effective strength of nematic fluctuation.

Now assume a finite SC gap $\Delta(\omega)$ is generated. Including Δ into the polarization function yields

$$\Pi(\Omega, \mathbf{q}) = 2N \sum_{s=\pm 1} \int \frac{d\omega}{2\pi} \int \frac{d^2\mathbf{k}}{(2\pi)^2} \frac{-A_1(\omega)A_1(\omega + \Omega)\omega(\omega + \Omega) + \xi_{\mathbf{k}}^s \xi_{\mathbf{k}+\mathbf{q}}^s - \Delta(\omega)\Delta(\omega + \Omega)}{\left[A_1^2(\omega)\omega^2 + (\xi_{\mathbf{k}}^s)^2 + \Delta^2(\omega) \right] \left[A_1^2(\omega + \Omega)(\omega + \Omega)^2 + (\xi_{\mathbf{k}+\mathbf{q}}^s)^2 + \Delta^2(\omega + \Omega) \right]}. \quad (35)$$

In principle, the polarization should also be coupled self-consistently to the DS equations for A_1 and Δ . This is in practice difficult to accomplish. Here, our strategy is to obtain an approximate analytical expression for the polarization. According to Appendix B, the exact polarization $\Pi(\Omega, \mathbf{q})$ can be perfectly replaced by the following simple function

$$\Pi(\Omega, \mathbf{q}) = N\gamma \frac{|\Omega|}{|q_y|} \frac{|\Omega|}{|\Omega| + 2.5\Delta'(0)}, \quad (36)$$

which reduces to Eq. (9) in the limit $\Delta'(0) = 0$. It is easy to observe that the above polarization is considerably smaller than Eq. (8). This indicates that the effective nematic fluctuation is strengthened once the SC gap is included in the polarization, which, as just mentioned, is due to the gap-induced suppression of fermion DOS.

The SC gap obtained by utilizing different approximations are presented in Fig. 6. It clearly shows that the magnitude of SC gap is visibly enhanced once the feedback effect of SC gap on the polarization is included.

D. Strong enhancement of superconductivity

We now analyze the interplay of two different pairing mechanisms. After long-term exploration, it has become clear that one single pairing interaction can hardly produce the observed high T_c of some cuprate and iron-based superconductors. Recently, there is a growing interest in the study of the cooperative effect of two distinct pairing interactions [24, 29, 39, 40]. However, the physical influence of such cooperation remains unclear due to the lack of a well-controlled framework to properly deal with the interplay of two pairing interactions.

We will apply the DS equation approach to compute the SC gap induced by the interplay between nematic fluctuation and additional short-ranged BCS coupling. Before carrying out calculations, it is useful to first make a qualitative analysis. As demonstrated in the last three subsections, the Yukawa coupling between fermions and nematic fluctuation is strongest at the QCP, and can lead to the largest SC gap. The Yukawa coupling could be made stronger if the polarization $\Pi(\Omega, \mathbf{q})$ is reduced. Now imagine a finite SC gap is already opened by weak BCS coupling, which might be mediated by the exchange of ordinary phonons. This gap can lower the low-energy fermion DOS. When the nematic fluctuation is introduced to the system, the effective strength of Yukawa coupling will be larger than the case in which no additional BCS coupling exists. Such scenario is similar to the feedback effect discussed in the last subsection. In actual materials, the interplay between quantum nematic fluctuation and electron-phonon interaction could combine to generate a greatly enhanced superconductivity that can never be realized by one single pairing interaction.

Here, we would like to mention that an analogous phenomenon occurs in graphene. It is known that the Coulomb interaction remains long-ranged despite the

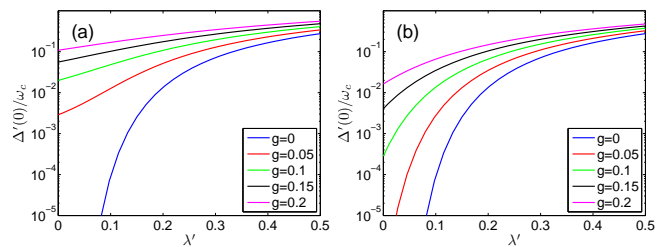


FIG. 5: Zero-energy SC gap $\Delta(0)$ obtained after including vertex correction: (a) $r' = 0$; (b) $r' = 1$. The results for $r' = 10$ and $r' = 100$ are nearly the same as those given in Fig. 2(c) and Fig. 2(d), and thus are not shown here.

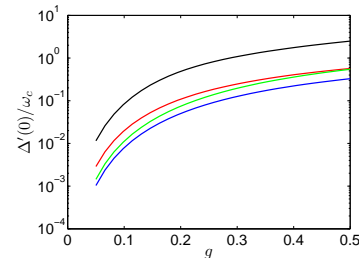


FIG. 6: Scaled gap obtained under various approximations. Blue: Vertex and feedback effect are neglected. Red: Vertex is included. Green: Feedback effect is included. Black: Both vertex and feedback effect are included.

presence of dynamical screening due to particle-hole excitations in graphene. When the Coulomb interaction is sufficiently strong, it can drive an excitonic pairing and open a finite dynamical gap, which turns the semimetal into an excitonic insulator [41–45]. For strictly gapless graphene, a dynamical excitonic gap is generated only when the Coulomb interaction strength α is larger than a critical value α_c [42–45]. Remarkably, if a bare gap is already opened for some reason, α_c is reduced to an arbitrarily small value [46] and the dynamical gap is also drastically amplified to a much larger value. The strong enhancement of excitonic pairing originates from the fact that the bare gap weakens the dynamical screening and increase the effective strength of Coulomb interaction.

The significant gap enhancement is firmly based on an important fact that the superposition of the gaps produced by two pairing interactions is highly nonlinear. Such nonlinear superposition plays an important role even when the feedback of SC gap to the Yukawa coupling is neglected. To precisely evaluate the total SC gap, the quantum nematic fluctuation and short-ranged BCS coupling should be treated in a self-consistent way. The DS equation offers a perfect framework for this study. After solving the DS equations, we find that the total gap can be much larger than the direct sum of the gap Δ_n generated by nematic fluctuation and the gap Δ_p generated by additional BCS coupling. We present the ratio $\Delta_B(0)/\Delta_A$ in Fig. 7, where $\Delta_B(0)$ denotes the total gap and $\Delta_A(0) = \Delta_n + \Delta_p$. We see that the ratio

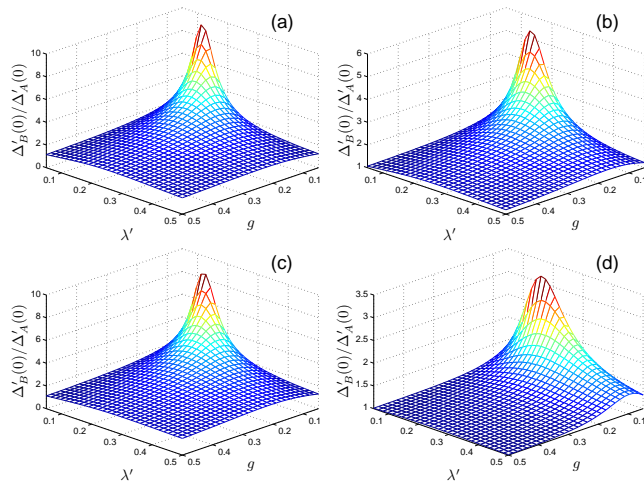


FIG. 7: Ratio $\Delta'_B(0)/\Delta'_A(0)$, where $\Delta'_B(0) = \Delta'(0)|_{\lambda',g}$ and $\Delta'_A(0) = \Delta'(0)|_{\lambda',g=0} + \Delta'(0)|_{\lambda'=0,g}$. (a) Vertex correction and feedback effect of finite SC gap on the polarization are neglected; (b) Vertex correction is included; (c) Feedback effect is included; (d) Both vertex correction and feedback effect are considered.

Δ_B/Δ_A ranges from unity to 10, depending on the values of model parameters and the approximation adopted to do the calculation. This ratio is computed under four different approximations, shown in Fig. 7(a)-(d). Comparing (a) to (d), we find that the ratio becomes smaller when both the vertex correction and feedback to polarization are incorporated. However, it is necessary to emphasize that the total gap $\Delta_B(0)$ obtained in the case of (d) is indeed much larger than that of case (a).

E. Impact of momentum dependence

In the above analysis, we entirely ignore the momentum dependence of $A_1(\varepsilon, p_y)$ and $\Delta(\varepsilon, p_y)$. In Appendix A, we show how to properly incorporate the momentum dependence in the coupled DS equations. After performing extensive numerical calculation, we confirm that our results are only slightly modified when the momentum dependence of $A_1(\varepsilon, p_y)$ and $\Delta(\varepsilon, p_y)$ is considered.

V. SUMMARY AND DISCUSSION

To summarize, our work presents a quantitative and self-consistent determination of the Landau damping rate and the s -wave SC gap in a 2D quantum critical NFL metal. This model system has potential applications to realistic unconventional superconductors, including cuprates, iron pnictides and FeSe. We demonstrate that the interplay of nematic fluctuation and a weak net attraction mediated leads to a significant enhancement of s -wave SC gap, which offers an efficient way to promote superconductivity. Since the magnitude of zero- T SC gap

is directly related to the SC transition temperature, the gap enhancement could lead to a remarkably increased T_c . This motivates us to conjecture that the observed high T_c of some cuprate and iron-based superconductors might originate from the mutual promotion of two distinct pairing mechanisms. Moreover, the total SC gap reaches its maximal value at the nematic QCP and is strongly suppressed as the system is tuned away from the QCP, hence a dome-shaped curve of T_c could be naturally produced, which appears to be in general agreement with experiments.

Our approach can be regarded as an extension of the BCS-Eliashberg theory to quantum critical metals in which the Landau damping is strong enough to invalidate the FL theory. Depending on the value of tuning parameter r , the non-SC system might stay in NFL regime, FL regime, or mixed FL/NFL regime that displays ordinary FL behavior at low energies and strong NFL behavior at high energies. Once Cooper pairing of (in)coherent fermions is realized, the system is in the SC state at low temperatures. Nevertheless, NFL behavior can still emerge in the intermediate energy range. Our approach thus provides a unified framework for the theoretic analysis of Cooper pairing in FL, NFL, and mixed FL/NFL metals.

The present work is restricted to zero temperature. The next step is to study the influence of finite temperature, and to accurately compute $T_c(r)$. This is not an easy problem because the quantum critical nematic fluctuation might lead to severe infrared divergence in the DS equations at nonzero temperature [28, 47]. It is also necessary to investigate the case in which the nematic order parameter has a finite mean value. The coexistence of nematic and SC orders might cause unusual effects that cannot occur in the disordered side of nematic QCP.

Another interesting future work is to apply the DS equation method to study the fate of superconductivity in correlated electron systems close to magnetic quantum phase transition. Such systems have direct applications to iron-based superconductors [8–10]. The magnetic order parameter is more complicated than nematic order parameter [48, 49] and the SC gap induced by magnetic fluctuation may have a d -wave symmetry, which makes DS equation analysis more involved. In some superconductors, the magnetic and nematic long-range orders are both important and indeed intrinsically connected [9, 50]. Despite such complications, one can always construct a set of coupled DS equations for the SC gap function and the renormalization factors, analyze the structure of the gap, determine the correlation between NFL behavior and Cooper pairing, and also examine whether the interplay of distinct pairing mechanisms lead to significantly enhanced superconductivity.

We would like to thank Jing Wang and Chun-Xu Zhang for very helpful discussions, and acknowledge the support by the National Natural Science Foundation of China under Grants 11574285 and 11504379.

-
- [1] J. Bardeen, L. Cooper, and J. R. Schrieffer, *Theory of Superconductivity*, Phys. Rev. **108**, 1175 (1957).
- [2] G. M. Eliashberg, *Interactions between Electrons and Lattice Vibrations in a Superconductor*, Sov. Phys. JETP **11**, 696 (1960).
- [3] A. A. Abrikosov, L. P. Gor'kov, and I. Y. Dzyaloshinskii, *Quantum Field Theoretical Methods in Statistical Physics* (Pergamon Press Inc., 1965).
- [4] H. Loehneysen, A. Rosch, M. Vojta, and P. Woelfle, *Fermi-Liquid Instabilities at Magnetic Quantum Phase Transitions*, Rev. Mod. Phys. **79**, 1015 (2007).
- [5] P. A. Lee, N. Nagaosa, and X.-G. Wen, *Doping a Mott Insulator: Physics of High-Temperature Superconductivity*, Rev. Mod. Phys. **78**, 17 (2006).
- [6] E. Fradkin, S. A. Kivelson, and J. M. Tranquada, *Colloquium: Theory of Intertwined Orders in High Temperature Superconductors*, Rev. Mod. Phys. **87**, 457 (2015).
- [7] B. Keimer, S. A. Kivelson, M. R. Norman, S. Uchida, and J. Zaanen, *From Quantum Matter to High-Temperature Superconductivity in Copper Oxides*, Nature **518**, 179 (2015).
- [8] A. Chubukov, *Pairing Mechanism in Fe-based Superconductors*, Ann. Rev. Condens. Matter Phys. **3**, 57 (2012).
- [9] R. M. Fernandes, A. V. Chubukov, and J. Schmalian, *What Drives Nematic Order in Iron-Based Superconductors?*, Nat. Phys. **10**, 97 (2014).
- [10] T. Shibauchi, A. Carrington, and Y. Matsuda, *A Quantum Critical Point Lying Beneath the Superconducting Dome in Iron Pnictides*, Ann. Rev. Condens. Matter Phys. **5**, 113 (2014).
- [11] H.-H. Kuo, J.-H. Chu, J. C. Palmstrom, S. A. Kivelson, and I. R. Fisher, *Ubiquitous Signatures of Nematic Quantum Criticality in Optimally Doped Fe-Based Superconductors*, Science **352**, 358 (2016).
- [12] A. Coldea and M. D. Watson, *The Key Ingredients of the Electronic Structure of FeSe*, arXiv:1706.00338v1.
- [13] S. Lederer, Y. Schattner, E. Berg, S. Kivelson, *Enhancement of Superconductivity near a Nematic Quantum Critical Point*, Phys. Rev. Lett. **114**, 097001 (2015).
- [14] Y. Schattner, S. Lederer, S. Kivelson, and E. Berg, *Ising Nematic Quantum Critical Point in a Metal: A Monte Carlo Study*, Phys. Rev. X **6**, 031028 (2016).
- [15] S. Lederer, Y. Schattner, E. Berg, and S. Kivelson, *Superconductivity and Non-Fermi Liquid Behavior near a Nematic Quantum Critical Point*, Proc. Natl. Acad. Sci. U.S.A. **114**, 4905 (2017).
- [16] M. Metlitski, D. Mross, S. Sachdev, and T. Senthil, *Cooper Pairing in Non-Fermi Liquids*, Phys. Rev. B **91**, 115111 (2015).
- [17] T. Maier and D. J. Scalapino, *Pairing Interaction near a Nematic Quantum Critical Point of a Three-Band CuO₂ Model*, Phys. Rev. B **90**, 174510 (2014).
- [18] M. Einenkel, H. Meier, C. Pépin, and K. B. Efetov, *Pairing Gaps near Ferromagnetic Quantum Critical Points*, Phys. Rev. B **91**, 064507 (2015).
- [19] S. Raghu, G. Torroba, and H. Wang, *Metallic Quantum Critical Points with Finite BCS Couplings*, Phys. Rev. B **92**, 205104 (2015).
- [20] H. Wang, S. Raghu, and G. Torroba, *Non-Fermi-Liquid Superconductivity: Eliashberg Approach versus the Renormalization Group*, Phys. Rev. B **95**, 165137 (2017).
- [21] Y. Wang, A. Abanov, B. L. Altshuler, E. A. Yuzbashyan, and A. V. Chubukov, *Superconductivity near a Quantum-Critical Point: The Special Role of the First Matsubara Frequency*, Phys. Rev. Lett. **117**, 157001 (2016).
- [22] I. Mandal, *Superconducting Instability in Non-Fermi Liquids*, Phys. Rev. B **94**, 115138 (2016).
- [23] P. T. Dumitrescu, M. Serbyn, R. T. Scalettar, and A. Vishwanath, *Superconductivity and Nematic Fluctuations in a Model of Doped FeSe Monolayers: Determinant Quantum Monte Carlo Study*, Phys. Rev. B **94**, 155127 (2016).
- [24] Z.-X. Li, F. Wang, H. Yao, and D.-H. Lee, *What Makes the T_c of Monolayer FeSe on SrTiO₃ So High: a Sign-Problem-Free Quantum Monte Carlo Study*, Sci. Bull **61**, 925 (2016).
- [25] Z.-X. Li, F. Wang, H. Yao, and D.-H. Lee, *Nature of the Effective Interaction in Electron-Doped Cuprate Superconductors: A Sign-Problem-Free Quantum Monte Carlo Study*, Phys. Rev. B **95**, 214505 (2017).
- [26] H. Yamase and R. Zeyher, *Superconductivity from Orbital Nematic Fluctuations*, Phys. Rev. B **88**, 180502(R) (2013).
- [27] T. Agatsuma and H. Yamase, *Structure of the pairing gap from orbital nematic fluctuations*, Phys. Rev. B **94**, 214505 (2016).
- [28] H. Wang, Y. Wang, and G. Torroba, *Superconductivity vs Quantum Criticality: Effects of Thermal Fluctuations*, arXiv:1708.04624v1.
- [29] D. Labat and I. Paul, *Pairing Instability near a Lattice-Influenced Nematic Quantum Critical Point*, Phys. Rev. B **96**, 195146 (2017).
- [30] A. E. Böhrer and A. Kreisel, *Nematicity, magnetism and superconductivity in FeSe*, arXiv:1711.06473v1.
- [31] F.-C. Hsu, J.-Y. Luo, K.-W. Yeh, T.-K. Chen, T.-W. Huang, P. M. Wu, Y.-C. Lee, Y.-L. Huang, Y.-Y. Chu, D.-C. Yan, and M.-K. Wu, *Superconductivity in the PbO-type structure α -FeSe*, Proc. Natl. Acad. Sci. U.S.A. **105**, 14262 (2008).
- [32] C.-L. Song, Y.-L. Wang, P. Cheng, Y.-P. Jiang, W. Li, T. Zhang, Z. Li, K. He, L. Wang, J.-F. Jia, H.-H. Hung, C. Wu, X. Ma, X. Chen, Q.-K. Xue, *Direct Observation of Nodes and Twofold Symmetry in FeSe Superconductor*, Science **331**, 1410 (2011).
- [33] V. Oganesyan, S. A. Kivelson, and E. Fradkin, *Quantum Theory of a Nematic Fermi Fluid*, Phys. Rev. **64**, 195109 (2001).
- [34] W. Metzner, D. Rohe, and S. Andergassen, *Soft Fermi Surfaces and Breakdown of Fermi-Liquid Behavior*, Phys. Rev. Lett. **91**, 066402 (2003).
- [35] L. Dell'Anna and W. Metzner, *Fermi Surface Fluctuations and Single Electron Excitations near Pomeranchuk Instability in Two Dimensions*, Phys. Rev. B **73**, 045127 (2006).
- [36] J. Rech, C. Pépin, A. V. Chubukov, *Quantum Critical Behavior in Itinerant Electron Systems: Eliashberg Theory and Instability of a Ferromagnetic Quantum Critical Point*, Phys. Rev. B **74**, 195126 (2006).
- [37] M. A. Metlitski and S. Sachdev, *Quantum Phase Transitions of Metals in Two Spatial Dimensions. I. Ising-Nematic Order*, Phys. Rev. B **82**, 075127 (2010).
- [38] T. Holder and W. Metzner, *Anomalous Dynamical Scal-*

- ing from Nematic and $U(1)$ Gauge Field Fluctuations in Two-Dimensional Metals, Phys. Rev. B **92**, 041112(R) (2015).
- [39] L. P. Gor'kov, *Peculiarities of Superconductivity in the Single-Layer FeSe/SrTiO₃ Interface*, Phys. Rev. B **93**, 060507(R) (2016).
- [40] J. Kang and R. M. Fernandes, *Superconductivity in FeSe Thin Films Driven by the Interplay between Nematic Fluctuations and Spin-Orbit Coupling*, Phys. Rev. Lett. **117**, 217003 (2016).
- [41] D. V. Khveshchenko, *Ghost Excitonic Insulator Transition in Layered Graphite*, Phys. Rev. Lett. **87**, 246802 (2001).
- [42] E. V. Gorbar, V. P. Gusynin, V. A. Miransky, and I. A. Shovkovy, *Magnetic Field Driven Metal-Insulator Phase Transition in Planar Systems*, Phys. Rev. B **66**, 045108 (2002).
- [43] G.-Z. Liu, W. Li, and G. Cheng, *Interaction and Excitonic Insulating Transition in Graphene*, Phys. Rev. B **79**, 205429 (2009).
- [44] J.-R. Wang and G.-Z. Liu, *Absence of Dynamical Gap Generation in Suspended Graphene*, New J. Phys. **14**, 043036 (2012).
- [45] M. E. Carrington, C. S. Fischer, L. v. Smekal, and M. H. Thoma, *Dynamical Gap Generation in Graphene with Frequency-Dependent Renormalization Affects*, Phys. Rev. B **94**, 125102 (2016).
- [46] C.-X. Zhang, G.-Z. Liu, and M.-Q. Huang, *Dynamical Fermion Mass Generation and Exciton Spectra in Graphene*, Phys. Rev. B **83**, 115438 (2011).
- [47] J.-R. Wang, G.-Z. Liu, and C.-J. Zhang, *Infrared Behavior of Dynamical Fermion Mass Generation in QED₃*, Phys. Rev. D **91**, 045006 (2015).
- [48] A. Abanov, A. V. Chubukov, and J. Schmalian, *Quantum-Critical Theory of the Spin-Fermion Model and Its Application to Cuprates: Normal State Analysis*, Adv. Phys. **52**, 119 (2003).
- [49] A. Abanov and A. V. Chubukov, *Anomalous Scaling at the Quantum Critical Point in Itinerant Antiferromagnets*, Phys. Rev. Lett. **93**, 255702 (2004).
- [50] K. Matsuura, Y. Mizukami, Y. Arai, Y. Sugimura, N. Maejima, A. Machida, T. Watanuki, T. Fukuda, T. Yajima, Z. Hiroi, K.Y. Yip, Y.C. Chan, Q. Niu, S. Hosoi, K. Ishida, K. Mukasa, S. Kasahara, J.-G. Cheng, S.K. Goh, Y. Matsuda, Y. Uwatoko, and T. Shibauchi, *Maximizing T_c by Tuning Nematicity and Magnetism in FeSe_{1-x}S_x Superconductors*, Nature Commun. **8**, 1143 (2017).

Appendix A: Influence of momentum dependence of

Here we examine whether the momentum dependence of A_1 and Δ play an important role. It is in principle to solve the self-consistent equations (23) and (23) numerically. Nevertheless, this is technically hard and extremely time-consuming. We choose to factorize the functions $A_1(\varepsilon, p_y)$ and $\Delta(\varepsilon, p_y)$ as follows:

$$A_1(\varepsilon, p_y) = A_1^a(\varepsilon)F_1(p_y), \quad (\text{A1})$$

$$\Delta(\varepsilon, p_y) = \Delta^a(\varepsilon)F_2(p_y), \quad (\text{A2})$$

where F_1 and F_2 satisfy

$$F_1(0) \equiv 1, \quad (\text{A3})$$

$$F_2(0) \equiv 1. \quad (\text{A4})$$

Accordingly, the self-consistent equations can be re-written as

$$A_1^a(\varepsilon)\varepsilon = \varepsilon + \frac{1}{2v} \int \frac{d\omega}{2\pi} \frac{dk_y}{2\pi} \frac{\Gamma(\varepsilon, 0; \omega, k_y) A_1^a(\omega) F_1(k_y) \omega}{\sqrt{(A_1^a(\omega))^2 F_1^2(k_y) \omega^2 + (\Delta^a(\omega))^2 F_2^2(k_y)}} D(\varepsilon - \omega, k_y), \quad (\text{A5})$$

$$A_1^a(\omega_c) F_1(p_y) \omega_c = \omega_c + \frac{1}{2v} \int \frac{d\omega}{2\pi} \frac{dk_y}{2\pi} \frac{\Gamma(\omega_c, p_y; \omega, k_y) A_1^a(\omega) F_1(k_y) \omega}{\sqrt{(A_1^a(\omega))^2 F_1^2(k_y) \omega^2 + (\Delta^a(\omega))^2 F_2^2(k_y)}} D(\omega_c - \omega, p_y - k_y), \quad (\text{A6})$$

$$\begin{aligned} \Delta^a(\varepsilon) &= \frac{\lambda}{2v} \int \frac{d\omega}{2\pi} \frac{dk_y}{2\pi} \frac{\Delta^a(\omega) F_2(k_y)}{\sqrt{(A_1^a(\omega))^2 F_1^2(k_y) \omega^2 + (\Delta^a(\omega))^2 F_2^2(k_y)}} \\ &+ \frac{1}{2v} \int \frac{d\omega}{2\pi} \frac{dk_y}{2\pi} \frac{\Gamma(\varepsilon, 0; \omega, k_y) \Delta^a(\omega) F_2(k_y)}{\sqrt{(A_1^a(\omega))^2 F_1^2(k_y) \omega^2 + (\Delta^a(\omega))^2 F_2^2(k_y)}} D(\varepsilon - \omega, k_y), \end{aligned} \quad (\text{A7})$$

$$\begin{aligned} \Delta^a(\omega_c) F_2(p_y) &= \frac{\lambda}{2v} \int \frac{d\omega}{2\pi} \frac{dk_y}{2\pi} \frac{\Delta^a(\omega) F_2(k_y)}{\sqrt{(A_1^a(\omega))^2 F_1^2(k_y) \omega^2 + (\Delta^a(\omega))^2 F_2^2(k_y)}} \\ &+ \frac{1}{2v} \int \frac{d\omega}{2\pi} \frac{dk_y}{2\pi} \frac{\Gamma(\omega_c, p_y; \omega, k_y) \Delta^a(\omega) F_2(k_y)}{\sqrt{(A_1^a(\omega))^2 F_1^2(k_y) \omega^2 + (\Delta^a(\omega))^2 F_2^2(k_y)}} D(\omega_c - \omega, p_y - k_y). \end{aligned} \quad (\text{A8})$$

By solving these equations, we have confirmed that the momentum dependence of A_1 and Δ can only play a minor role. The zero-energy gap $\Delta'(0)$ obtained in the presence and absence of such momentum dependence are nearly the same.

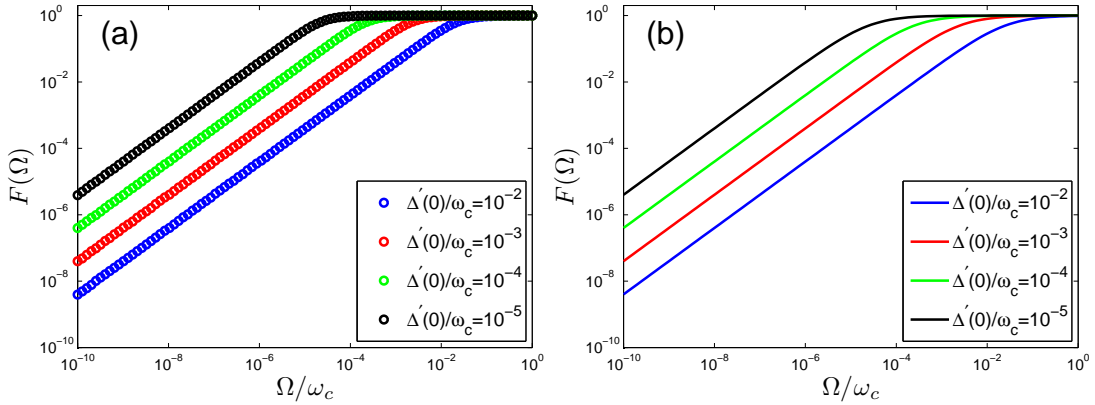


FIG. 8: (a) Numerical results for $F(|\Omega|)$ with different values $\Delta'(0)$; (b) The analytical expression $F(|\Omega|) = \frac{|\Omega|}{|\Omega| + 2.5\Delta'(0)}$ with different values of $\Delta'(0)$.

Appendix B: Including gap in the polarization

Including the feedback effect of finite SC gap, the polarization takes the following form

$$\begin{aligned} \Pi(\Omega, \mathbf{q}) = & 2N \sum_{s=\pm 1} \int \frac{d\omega}{2\pi} \int \frac{d^2\mathbf{k}}{(2\pi)^2} \\ & \times \frac{-A_1(\omega)A_1(\omega + \Omega)\omega(\omega + \Omega) + \xi_{\mathbf{k}}^s \xi_{\mathbf{k}+\mathbf{q}}^s - \Delta(\omega)\Delta(\omega + \Omega)}{\left[A_1^2(\omega)\omega^2 + (\xi_{\mathbf{k}}^s)^2 + \Delta^2(\omega) \right] \left[A_1^2(\omega + \Omega)(\omega + \Omega)^2 + (\xi_{\mathbf{k}+\mathbf{q}}^s)^2 + \Delta^2(\omega + \Omega) \right]}. \end{aligned} \quad (\text{B1})$$

Performing the integration of momentum, we obtain

$$\Pi(\Omega, \mathbf{q}) = \frac{N\gamma}{2|q_y|} \int d\omega \frac{-A_1(\omega)A_1(\omega + \Omega)\omega(\omega + \Omega) - \Delta(\omega)\Delta(\omega + \Omega)}{\sqrt{A_1^2(\omega)\omega^2 + \Delta^2(\omega)} \sqrt{A_1^2(\omega + \Omega)(\omega + \Omega)^2 + \Delta^2(\omega + \Omega)}}. \quad (\text{B2})$$

In the limit of $\Omega = 0$ and $\Delta = 0$, the polarization is simplified to

$$\Pi(\Omega = 0, \mathbf{q}, \Delta = 0) = N\gamma \frac{1}{2|q_y|} \int d\omega (-1). \quad (\text{B3})$$

For the polarization to satisfy the condition $\Pi(\Omega = 0, \mathbf{q}, \Delta = 0) = 0$, we employ the redefinition

$$\Pi(\Omega, \mathbf{q}) - \Pi(\Omega = 0, \mathbf{q}, \Delta = 0) \rightarrow \Pi(\Omega, \mathbf{q}), \quad (\text{B4})$$

and then obtain

$$\Pi(\Omega, \mathbf{q}) = N\gamma \frac{1}{2|q_y|} \int d\omega \left[1 - \frac{A_1(\omega)A_1(\omega + \Omega)\omega(\omega + \Omega) + \Delta(\omega)\Delta(\omega + \Omega)}{\sqrt{A_1^2(\omega)\omega^2 + \Delta^2(\omega)} \sqrt{A_1^2(\omega + \Omega)(\omega + \Omega)^2 + \Delta^2(\omega + \Omega)}} \right]. \quad (\text{B5})$$

It can be further written as

$$\Pi(\Omega, \mathbf{q}) = N\gamma \frac{|\Omega|}{|q_y|} F(|\Omega|), \quad (\text{B6})$$

where

$$\begin{aligned} F(|\Omega|) = & \frac{1}{|\Omega|} \int_0^{+\infty} d\omega \left[1 - \frac{A_1(\omega)A_1(\omega + |\Omega|)\omega(\omega + |\Omega|) + \Delta(\omega)\Delta(\omega + |\Omega|)}{\sqrt{A_1^2(\omega)\omega^2 + \Delta^2(\omega)} \sqrt{A_1^2(\omega + |\Omega|)(\omega + |\Omega|)^2 + \Delta^2(\omega + |\Omega|)}} \right] \\ & + \frac{1}{2|\Omega|} \int_0^{|\Omega|} d\omega \left[1 - \frac{-A_1(\omega)A_1(\omega - |\Omega|)\omega(\omega - |\Omega|) + \Delta(\omega)\Delta(\omega - |\Omega|)}{\sqrt{A_1^2(\omega)\omega^2 + \Delta^2(\omega)} \sqrt{A_1^2(\omega - |\Omega|)(\omega - |\Omega|)^2 + \Delta^2(\omega - |\Omega|)}} \right]. \end{aligned}$$

Under the approximation $A_1(\omega) \approx A_1(0)$ and $\Delta(\omega) \approx \Delta(0)$, we get

$$\begin{aligned} F(|\Omega|) = & \frac{1}{|\Omega|} \int_0^{+\infty} d\omega \left[1 - \frac{\omega(\omega + |\Omega|) + \Delta'^2(0)}{\sqrt{\omega^2 + \Delta'^2(0)} \sqrt{(\omega + |\Omega|)^2 + \Delta'^2(0)}} \right] \\ & + \frac{1}{2|\Omega|} \int_0^{|\Omega|} d\omega \left[1 - \frac{-\omega(\omega - |\Omega|) + \Delta'^2(0)}{\sqrt{\omega^2 + \Delta'^2(0)} \sqrt{(\omega - |\Omega|)^2 + \Delta'^2(0)}} \right], \end{aligned} \quad (\text{B7})$$

where $\Delta'(0) = \frac{\Delta(0)}{A_1(0)}$. The numerical result is shown in Fig. 8, which indicates that $F(|\Omega|)$ can be accurately approximated by the expression

$$F(|\Omega|) = \frac{|\Omega|}{|\Omega| + 2.5\Delta'(0)}. \quad (\text{B8})$$